Endocrine (2019) 65:61–72
https://doi.org/10.1007/s12020-019-01940-x

ORIGINAL ARTICLE

Check for updates

Phenotypic characterization of a novel type 2 diabetes animal model in a SHANXI MU colony of Chinese hamsters

Lu Wang[1,2] · Chenyang Wang[1,2] · Ruihu Zhang[1,2] · Yu Liu[3] · Chunfang Wang[1,2] · Guohua Song[1,2] · Jingjing Yu[1,2] · Zhaoyang Chen[1,2]

Received: 12 December 2018 / Accepted: 17 April 2019 / Published online: 25 April 2019

Abstract

Purpose Developing animal models for human diseases is critical for studying complex diseases such as type 2 diabetes mellitus (T2DM). Since inbred colonies of Chinese hamsters tend toward spontaneous development of diabetes, we investigated them as a possible model.

Methods We regarded individuals with fasting blood glucose (FBG) higher than 6.0 mmol/L and post-prandial blood glucose (PBG) higher than 7.0 mmol/L as diabetic based on the mean and 95% frequency distribution values of FBG and PBG. Diabetic hamsters were characterized based on metabolic profiles, histopathological features, and changes in the expression of genes involved in glucose and lipid metabolism.

Results Metabolic analyses showed that diabetic hamsters exhibited mild hyperglycemia, hypertriglyceridemia, glucose intolerance, and insulin resistance. Histopathological analysis revealed that cell nuclei migrated inward in skeletal muscle and obvious partial liver lipid deposition and focal necrosis was found. We additionally observed mild injury, atrophy, and occasional vacuolization in islet cells. Changes in the expression of several genes related to glucose and lipid metabolism were observed. Decreased expression of adiponectin and GLUT4 and increased expression of PPARγ, Akt, and leptin was observed in skeletal muscle. Decreased expression of adiponectin with increased expression of PPARγ and leptin was observed in the liver.

Conclusions These results indicate that we have established a spontaneous diabetic hamster line that closely mimics human T2DM, which may hold potential for further research on the pathogenesis and treatment of this disease.

Keywords Chinese hamster · Differentially expressed genes · Glucose intolerance · Insulin resistance · Type 2 diabetes mellitus

Introduction

Diabetes is considered a complex endocrine metabolic disease, primarily characterized by hyperglycemia, subject to multiple susceptibility genes and environmental factors [1, 2]. In recent years, the global prevalence of diabetes has been increasing, with a projected increase from 451 million patients in 2017 to 693 million by 2045 [3]. Among the different forms of diabetes, type 2 diabetes mellitus (T2DM) accounts for over 90% of diagnosed patients and constitutes a serious threat to human health [4]. However, because of its complex etiology, the underlying molecular mechanisms for some aspects of human T2DM remain to be described [5, 6]. This poses serious challenges and difficulties for identifying therapeutic targets and prognostic indicators for the disease [7, 8]. Therefore, a meaningful animal model with clinical features similar to human T2DM is critical for future study.

Supplementary information The online version of this article (https://doi.org/10.1007/s12020-019-01940-x) contains supplementary material, which is available to authorized users.

✉ Zhaoyang Chen
ccytycn@163.com

[1] Laboratory Animal Center of Shanxi Medical University, Shanxi Province, China

[2] Shanxi Key Laboratory of Experimental Animal Science and Animal Model of Human Disease, Shanxi Medical University, Shanxi Province, China

[3] Department of Pharmacology, Shanxi Medical University, Shanxi Province, China

Existing T2DM animal models include spontaneous models based on genetic predisposition or experimentally induced models whereby chemical agents, dietary changes, genetic modifications, or a combination of these factors are used to cause disease [9]. Experimentally induced animal models are often established by injecting drugs (alloxan or streptozotocin) or provisioning with high-fat diets [10]. The dose and composition of diets affect the pathogenesis of diabetes, and the chemicals used to induce diabetes can cause severe dose-dependent damage to β cells, while lower doses may fail to induce diabetes [10, 11]. Genetic animal models are valuable tools for the study of genetic factors contributing to T2DM [6], particularly when both pathogenesis and metabolic characteristics are similar to those observed in humans. However, only a few polygenic animal models have thus far been developed [12]. Existing rodent models have characteristics applicable to specific conditions, such as Nagoya-Shibata-Yasuda (NSY) mice [13], Tsumura-Suzuki obese diabetes (TSOD) mice [14], TALLYHO/Jng (TH) mice [15], and Mongolian gerbils [4, 16]. These models exhibit varying degrees of obesity and are resources for understanding the genetic causes of obese T2DM, but they are not good representatives of non-obese T2DM. Goto-Kakizaki (GK) rats [17] are a non-obese animal model of T2DM, but are characterized by deficient insulin secretion, and are therefore not suitable for studying T2DM caused by insulin resistance. As such, non-obese insulin-resistant T2DM is not currently represented by a non-induced animal model.

In human clinical cases, T2DM manifests with insulin resistance and defects in glucose utilization. Insulin resistance is a chronic inflammatory condition, closely linked to cytokines secreted by adipose tissue such as leptin, adiponectin, resistin, and others [18]. Peroxisome proliferator-activated receptors (PPARs) are the main regulators of adipocytokines. Among these, PPARγ plays a valuable role in adipocyte differentiation and glucose metabolism [19, 20]. Alteration in PPARγ expression or its mutation may induce insulin resistance and/or affect basal glucose uptake in peripheral tissues [19, 21]. Insulin-sensitive peripheral tissues, such as skeletal muscle and adipose tissue, contain at least two different glucose transporter isoforms, glucose transporter (GLUT)-1 and GLUT4, which participate in glucose uptake [22], of which GLUT4 is the major insulin-regulated transporter [22, 23]. In addition, the phosphatidylinositol 3-kinase/protein kinase B (PI3K/Akt) signal transduction pathway is associated with GLUT4 translocation, which is regulated by insulin stimulation [24]. In contrast, GLUT2 is not dependent upon insulin action and mediates plasma glucose uptake in hepatocytes [25].

Chinese hamsters were first reported as a potential diabetic model in 1963 when they were found to have developed spontaneous diabetes in their colony after four to five generations of inbreeding [26–28]. One strain of these hamsters, an inbred sub-line called SHANXI MU, was recently developed using selective breeding to display non-obese hyperglycemia with slightly increased fasting blood glucose (FBG). In the present study, we characterized the diabetic phenotypes of these hamsters by monitoring levels of glucose, lipids, and insulin in the blood, and by analyzing pathological features in the pancreas, liver, and skeletal muscle. In addition, we investigated mRNA and protein expression in liver and skeletal muscle of five genes related to glucose and lipid metabolism, including *Lep*, *Adipoq*, *Glut4*, *Pparg*, and *Akt*. An understanding of the underlying metabolic characteristics of Chinese hamsters could provide the basis for new insights into the molecular pathogenesis of T2DM in this hamster strain, as well as contribute to further understanding of T2DM in general.

Materials and methods

Animals and housing

Chinese hamsters (license number: SCXK2015-001) were bred and maintained at the Center for Experimental Animals of Shanxi Medical University. Animals were individually housed in wire cages (40 × 20 × 30 cm) with sawdust bedding and were kept under standard laboratory conditions at 22 ± 2 °C, 50–70% humidity, and 12/12-h light/dark cycle with free access to sterile food and water. All experimental procedures of this study were approved by the Experimental Animal Ethics Committee of Shanxi Medical University.

Selective inbreeding of diabetic Chinese hamsters

Beginning at the age of 3 months, FBG and post-prandial blood glucose (PBG) levels of hamsters were measured by an Accu-Chek Active Blood Glucose Meter (Roche Diagnostics GmbH, Germany) once a month for 1 year. Based on the mean value and the 95% frequency distribution of FBG and PBG values, we regarded individuals having FBG ≤ 4.5 mmol/L and PBG < 6.0 mmol/L as non-diabetic control animals and individuals having FBG ≥ 6.0 mmol/L and PBG > 7.0 mmol/L as diabetic. One litter of eight individuals contained three hamsters (one female and two males) that met the criteria for hyperglycemia at the age of 23 weeks. These three hamsters were designated as the parent generation for production of a diabetic line. Following their mating, we measured FBG and PBG of their offspring from F1–F7 generations and chose individuals showing signs of diabetes for brother–sister or backcrossed mating. Body weight was measured from 4 weeks of age for

all individuals. Nasal–anal length was also measured at 12, 24, 36, and 48 weeks, and body mass index (BMI) was calculated as body weight (g) divided by the square of nasal–anal length (cm). After body weight and blood glucose stabilized, 48-week-old hamsters were selected for metabolic index detection and pathological analysis.

Glucose metabolism assay: oral glucose tolerance test (OGTT)

OGTT was performed after a 12-h fast. Hamsters were given glucose orally (10 g/kg) via a gavage needle. After glucose administration, blood glucose content was measured at 0, 30, 60, and 120 min from the tail tip using an Accu-Chek Active Blood Glucose Meter. Blood samples (200 μL) were drawn from the retro-orbital sinus at 0, 15, 30, and 60 min, clotted for 30 min, and centrifuged for 20 min at 4 °C and 1300 g. Serum was collected for insulin measurement using an ELISA kit (Millipore, USA). Using these measures, we then applied the trapezoidal rule to calculate the area under the curve (AUC) [29].

Lipid metabolism assay: serum triglyceride (TG) and total cholesterol (TC) content

Animals were fasted for 12 h, and 400 μL of blood was drawn from the retro-orbital sinus, clotted for 1 h, and centrifuged for 20 min at 4 °C and 1300 *g*. Serum was collected and stored at −20 °C. Levels of TG and TC were measured using an automatic biochemical analyzer (Hitachi 7020, Japan).

Insulin content and insulin tolerance test (ITT)

Concentrations of fasting serum insulin were measured using an ELISA kit (Millipore, USA). The optical density (OD) of each well was determined using a microplate reader (BioTek, USA) equipped with a 450 nm wavelength filter. Statistical analyses were performed comparing the mean values of each set of duplicate wells. We then calculated a homeostasis model assessment of insulin resistance (HOMA-IR) as [fasting insulin (μU/mL) × fasting glucose (mmol/L)]/22.5.

ITT was performed after 5 h of fasting. Hamsters were given insulin (Novolin, China) by intraperitoneal injection (0.75 IU/kg). After insulin administration, blood glucose was measured at 0, 30, 60, 120, and 180 min at the tail tip using a blood glucose meter.

HbA1c content and determination assay

Animals were fasted for 12 h and 100 μL of blood was collected from the retro-orbital sinus and stored in a centrifuge tube containing EDTA to prevent coagulation. The concentrations of HbA1c were measured using glycosylated hemoglobin Alc assay kits (Nanjing Jiancheng Bio Inc., China). HbA1c (700 nm) levels were expressed as percentage concentration.

Body composition and metabolism assay

Hamsters were anesthetized by intraperitoneal injection of 50 mg/kg pentobarbitone sodium (Sigma, USA). Body composition, including body mass, bone mineral content (BMC), total fat mass, lean mass, bone mineral density (BMD), and the percentage of fat distributed in tissue, was detected using an InAlyzer Dual Energy X-ray Animal Body Composition Analysis System (Medikors Inc., Korea). Daily food and water consumption were measured using an Oxymax Lab Animal Monitoring System (Columbus Instruments Inc., USA).

Histological analysis and liver glycogen content assay

At the end of the experiment, hamsters were euthanized with an overdose of pentobarbitone sodium by intraperitoneal injection. Skeletal muscle and pancreatic, and liver tissues were collected, and divided into three and four portions, respectively. One portion was used for histopathological analysis and two were stored at −80 °C used for quantitative real-time PCR and western blot analysis. In addition, another portion of fresh liver tissue for hepatic glycogen detection was taken, according to the instruction manual of liver glycogen assay kits (Nanjing Jiancheng Bio Inc., China).

For histopathological analysis, tissues were first fixed in 4% paraformaldehyde for about 48 h. These were then dehydrated, embedded in paraffin, cut into 4 μm slices, placed on glass slides, and stained with hematoxylin and eosin (HE). Frozen sections of liver tissue were also stained with Sudan III dye. These were then observed using a microscope.

Leptin, adiponectin, GLUT4, PPARγ, and Akt mRNA abundance assays

Total RNA in skeletal muscle and liver was extracted using Trizol Reagent (Takara Bio Inc., Japan) from control and diabetic hamsters. Complementary DNA was synthesized using 2 μg of total RNA in a 20 μL reaction mixture using PrimeScript™ RT Master Mix (Perfect Real-Time) Kit (Takara Bio Inc., Japan). Real-time PCR was performed in a StepOnePlus RT-PCR system (Applied Biosystems, USA) using a SYBR® Premix Ex Taq™ II (Tli RNaseH Plus) Kit (Takara Bio Inc., Japan). PCR conditions consisted of one cycle of denaturation at 95 °C for 30 s, followed by 40

cycles of denaturation at 95 °C for 5 s with annealing and extension at 60 °C for 30 s. A reaction melting curve analysis was performed to verify the specificity of the amplified products. Gene expression relative to β-actin mRNA was calculated. Specific primers were designed using Primer 5.0 software, which were synthesized by TaKaRa (Takara Bio Inc., Japan) (Table 1).

Immunohistochemical analysis

To detect levels of insulin in the pancreas and GLUT4 in the liver, we cut the tissue of interest into 4 μm slices and placed them on glass slides. Immunohistochemistry was performed with insulin (1:200 dilution; Boster, China), GLUT4 (1:300 dilution; ABclonal, China), and secondary biotin-conjugated antibody (Boster, China). We observed the dye distribution and intensity in immunostained tissues, then calculated mean ODs using a fluorescence microscope with a DP70 digital imaging system (Olympus, Japan) and Image-Pro Plus 6.0 (Media Cybernetics, USA).

Total protein extraction and western blot analysis

Total protein in skeletal muscle and liver was extracted using a protein extraction kit (Boster, China). Concentration of total protein was measured using a bicinchoninic acid (BCA) kit (Boster, China). Each protein sample was separated by sodium dodecyl sulfate–polyacrylamide gel electrophoresis and transferred to a nitrocellulose (NC) membrane. After blocking with 5% nonfat milk, the NC membrane was incubated overnight at 4 °C with the following primary antibodies: leptin (1:400 dilution; Boster, China), ADIPOQ (1:1000 dilution; ABclonal, China), GLUT4 (1:1000 dilution; Boster, China), AKT (1:400 dilution; Boster, China), PPARγ (1:1000 dilution; ABclonal, China), GLUT2 (1:1000 dilution; ABclonal, China), and β-actin (1:1000 dilution; Bioworld, China). Following this, the NC membrane was washed and incubated for 1 h at room temperature with horseradish peroxidase-conjugated goat anti-rabbit or anti-mouse IgG antibody (1:4000 dilution; Bostser, China). The immunoreactive band was detected by enhanced chemiluminescence and quantified using a chemiluminescence imaging system (G:Box Chemi XX9, UK).

Table 1 PCR primer sequences and corresponding sizes

Gene	Primers (5′-3′)	Sizes (bp)
β-actin	F: 5′-AGCCATGTACGTAGCCATCC-3′	20
	R: 5′-ACCCTCATAGATGGGCACAG-3′	20
Adipoq	F: 5′-GGACAAGGCTGTTCTCTTCACC-3′	22
	R: 5′-ATCCCCATCCCCATACACC-3′	19
Glut4	F: 5′-ATCCCACAAGGCACTCTCACTAC-3′	23
	R: 5′-GCCAGCATAGCCCTTTTCC-3′	19
Pparg	F: 5′-GGAGCCTAAGTTTGAGTTTGCTGTG-3′	25
	R: 5′-TGCAGCAGGTTGTCTTGGATG-3′	21
Akt	F: 5′-GCCTGCCCTTCTACAACCA-3′	19
	R: 5′-GCCTCTGTGTGGGGTCTTTC-3′	20

Statistical analysis

All data were analyzed using SPSS 16.0 software (IBM, USA). Student's *t*-test was used to compare control and diabetic groups. One-way analysis of variance was used to compare FBG, PBG, BMI, HOMA-IR, and TG between the control and diabetic groups at the indicated weeks. To evaluate differences in the incidence of diabetes, the chi-squared test was used. Results are presented as mean ± standard deviation. *P*-values < 0.05 were considered statistically significant.

Results

Establishment of diabetic Chinese hamsters

As the number of breeding generations increased, the incidence of diabetes gradually increased (Fig. 1). In the F7 generation hamsters, the total incidence was 36.73%, twice as high as that F1 hamsters (Fig. 1a), but this difference was not statistically significant. In addition, significant differences in the incidence of diabetes were not observed between the F3 to F6 generations and the F1 generation. There was also no significant difference in the incidence of diabetes between males and females (Fig. 1a). Individual onset of hyperglycemia varied, with the earliest onset occurring at 15 weeks of age and some as late as 37 weeks. With increasing age, FBG and PBG values gradually increased (Fig. 1b, c), which means that hamsters spontaneously developed diabetes in an age-dependent manner. The FBG values of diabetic hamsters were significantly higher than those of the control group at the age of 12, 24, 36, and 48 weeks (Fig. 1b). The PBG values were significantly higher in diabetic hamsters compared with those in the control at the age of 24, 36, and 48 weeks (Fig. 1c). Further, compared with 12-week-old hamsters, FBG values in control and diabetic hamsters (Fig. 1b), and PBG values in diabetic group hamsters (Fig. 1c) were higher at 48 weeks of age. We therefore focused our studies on hamsters at 48 weeks of age; 15 males and 15 females of this age were randomly selected from each experimental group.

Clinical features

Male hamsters began to gain weight faster than females from the age of 6 weeks in experimental groups (Fig. 2a). Within gender, there was no difference between the control and diabetic groups (Fig. 2a). A significant decrease in BMI was observed in both male and female diabetic individuals at 48 weeks (Fig. 2b). At this point, total daily food intake significantly increased in diabetic individuals (Fig. 2c), and while total water intake also showed an increasing trend, this was not significantly different from the control group (Fig. 2d). Body composition analysis showed that the total per-

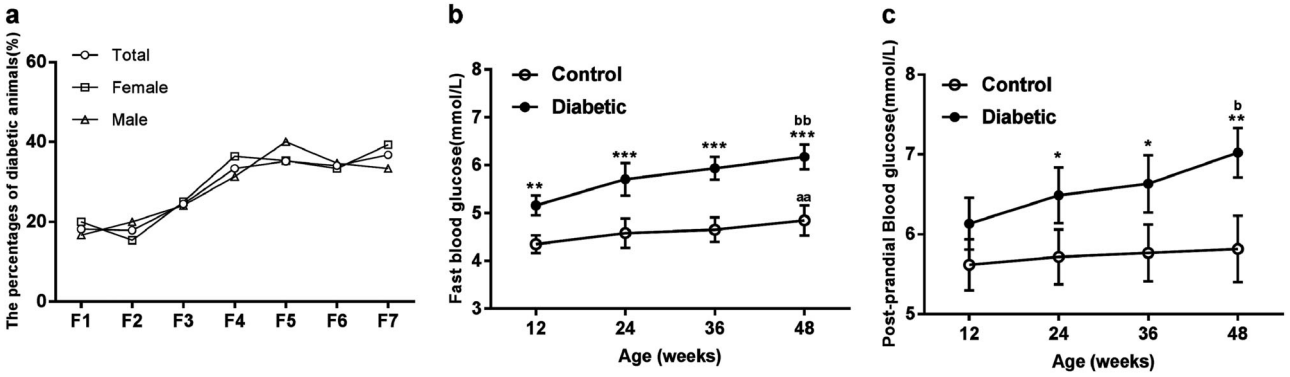

Fig. 1 Incidence of diabetes in each generation and fasting blood glucose (FBG), post-prandial blood glucose (PBG) at 12, 24, 36, and 48 weeks in Chinese hamster. **a** Percentages of diabetes animals with FBG ≥ 6.0 mmol/L and PBG > 7.0 mmol/L in male, female and total hamsters from F1 to F7. **b**, **c** FBG and PBG at 12, 24, 36, and 48 weeks (control, $n = 30$; diabetic, $n = 15$). Statistical differences were analyzed by independent samples *t*-test. Data are shown as mean ± SD. Diabetic vs. Control: $^{*}P < 0.05$, $^{**}P < 0.01$, $^{***}P < 0.001$. $^{aa}P < 0.01$ vs. 12 weeks in control group, $^{b}P < 0.05$ vs. 12 weeks in diabetic group, $^{bb}P < 0.01$ vs. 12 weeks in diabetic group

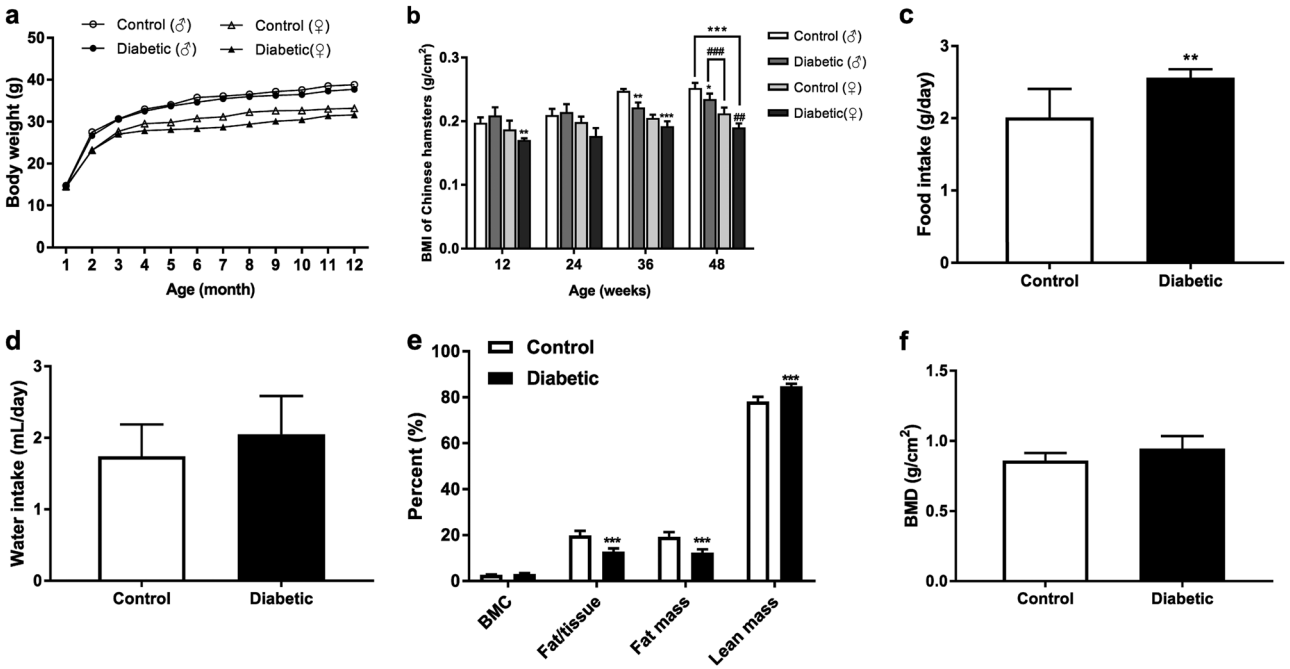

Fig. 2 Body weight, BMI, food intake, water consumption and body composition in Chinese hamster. **a** Body weight in male and female hamsters in both control ($n = 38$) and diabetic ($n = 25$) groups. **b** Body mass index (BMI) was calculated as body weight (g) divided by the square of the anal–nasal length (cm) at the indicated ages in both control ($n = 38$) and diabetic ($n = 25$) groups. Mean daily food intake **c** and water consumption **d** were measured at the indicated ages. The body composition, including bone mineral content (BMC), fat mass, lean mass, percent fat in tissue **e** and bone mineral density (BMD) **f**, were measured by the InAlyzer dual-energy X-ray animal body composition analysis system. The percentages of BMC, fat mass and lean mass were also calculated. e Statistical differences were analyzed by the independent-samples *t*-test. Data are shown as mean ± SD. Control, $n = 12$; diabetic, $n = 14$. In **b**, $^{*}P < 0.05$, $^{**}P < 0.01$ and $^{***}P < 0.001$ vs. male hamsters of the control group; $^{\#\#}P < 0.01$ and $^{\#\#\#}P < 0.001$ vs. female hamsters of the control group. In **c** and **e**, $^{**}P < 0.01$ and $^{***}P < 0.001$ vs. control

centage of fat mass and the percentage of fat distributed within tissues were considerably lower in diabetic individuals (Fig. 2e). It is worth noting that the proportion of fat in tissues decreased by 37% in diabetic hamsters. Contrastingly, in the diabetic group, the percentage of lean mass was significantly greater. There were no obvious differences in BMD (Fig. 2f) or percent BMC (Fig. 2e) between the control and diabetic groups. These data indicated that this hamster strain spontaneously developed non-obese T2DM.

Metabolic parameters: FBG, PBG, serum lipid (TC, TG), HbA1c, insulin, HOMA-IR, and liver glycogen

Measures of FBG, PBG, TG, insulin, HOMA-IR, and liver glycogen levels in diabetic hamsters were all significantly higher than they were in the controls (Table 2). Among them, FBG and PBG values were not significantly different between control and diabetic hamsters before the age of 12 weeks (Online Resource 1a, b). At the age of 36 weeks, the values of HOMA-IR and TG began to significantly increase in diabetic hamsters compared with the control group (Online Resource 1c, d). Serum TC in the diabetic group exhibited an increasing trend, but this was not statistically significant compared with the control group (Table 2). The level of HbA1c, a long-term marker for hyperglycemia, showed more than a 1.3-fold increase in the diabetic group (Table 2). These results indicated that the diabetic hamsters used in this study exhibited insulin resistance and metabolic disease.

OGTT and ITT assays

Impaired glucose tolerance in diabetic hamsters was evident at the 30-min time point of the OGTT (9.93 ± 1.63 versus 14.43 ± 3.25 mmol/L; Fig. 3a). Accordingly, the AUC increased by 40% in diabetic hamsters (Fig. 3b). These results indicated marked impairment in glucose tolerance. After glucose loading, the serum insulin level of the hamsters showed similar increases in control and diabetic groups from 0 to 15 min (Fig. 3c). At 30 min, the control group showed significantly lower measures, whereas serum insulin levels remained high in diabetic hamsters (Fig. 3c). Insulin AUC (Fig. 3d) was also significantly higher in the diabetic group. This suggested that diabetic hamsters had defective glucose-stimulated insulin secretion.

To further evaluate the contribution of insulin resistance, we also measured changes in the blood glucose of diabetic hamsters in response to exogenous insulin. Exogenous insulin treatment induced a rapid reduction in blood glucose within 30 min in control hamsters, followed by gradual return to euglycemia over 120 min (Fig. 3e). Although low blood glucose level was also observed in the diabetic group in the first 30 min after recombinant human insulin injection, it was ultimately maintained at a higher level (Fig. 3e). These data indicated that these diabetic hamsters exhibited impaired glucose intolerance and insulin resistance.

Pathological analysis of the diabetic target organs

Microscopic analysis of stained slides showed inward migration of cell nuclei in the skeletal muscle of diabetic hamsters (Fig. 4a). Partial liver steatosis and focal necrosis were also observed (Fig. 4b). Further Sudan III staining of liver showed a deposition of lipids in the diabetic group (Fig. 4c).

Pancreatic tissue of the control group showed normal lobular architecture, with islet cells morphologically identical and evenly distributed (Fig. 4d). In contrast, mild injury and abnormal distribution of islet cells, partial nuclear shrinkage, and occasional vacuolization were observed in the diabetic group (Fig. 4d). We also examined insulin expression by immunohistochemistry analysis. In the control group, insulin was evenly distributed and relatively abundant. The distribution of insulin in the diabetic group was not uniform, and insulin granules could be clearly seen after staining (Fig. 4e, f). This suggested continuous, potent stimulation of insulin secretion in diabetic hamsters.

Analysis of candidate diabetic gene expression in liver and skeletal muscle

We found that the expression of level adiponectin, based on observations of both mRNA and protein levels, was significantly lower in diabetic hamsters (Fig. 5a, b). Expression of GLUT4 varied in different tissues. In the skeletal muscle

Table 2 The metabolic parameters of Chinese hamster in control and diabetic group

Groups	FBG (mmol/L)	PBG (mmol/L)	TC (mmol/L)	TG (mmol/L)	HbA1c (%)	Insulin (μU/mL)	HOMA-IR	Liver glycogen content (mg/g)
Control ($n = 14$)	3.96 ± 0.16	5.81 ± 0.42	4.29 ± 0.54	1.84 ± 0.65	6.57 ± 1.12	36.25 ± 8.27	6.31 ± 1.29	2.16 ± 0.28
Diabetic ($n = 12$)	6.90 ± 0.37***	7.85 ± 0.63**	4.58 ± 0.55	2.66 ± 0.62***	9.16 ± 1.46***	52.15 ± 13.05*	14.78 ± 3.51***	3.96 ± 0.70***

Data are mean ± standard deviations (SD)

FBG fasting blood glucose, *PBG* post-prandial blood glucose, *TC* total cholesterol, *TG* triglyceride, *HbAlc* glycosylated hemoglobin Alc, *HOMA-IR* homeostasis model assessment of insulin resistance, *HOMA-IR* fasting insulin (μU/mL) × fasting blood glucose (mmol/L)/22.5

Results from Student's *t*-test. Diabetic vs. Control: $^{*}P < 0.05$, $^{**}P < 0.01$, $^{***}P < 0.001$

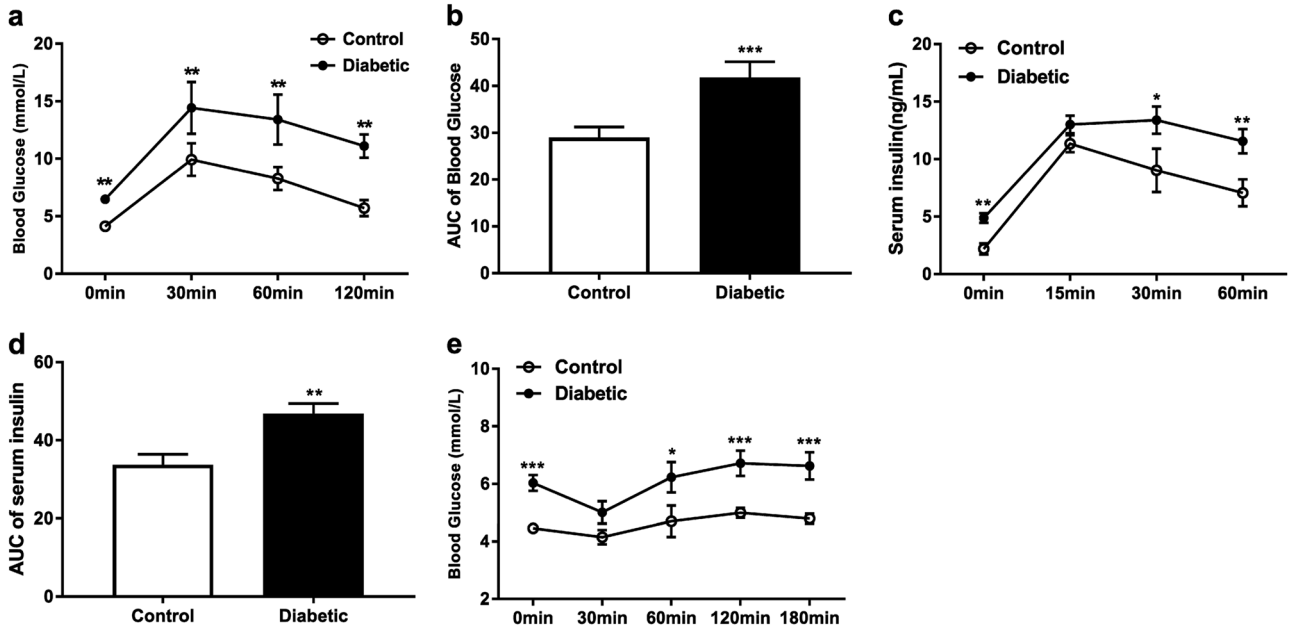

Fig. 3 Oral glucose tolerance test (OGTT), insulin secretion and insulin tolerance test (ITT) between control and diabetic group in Chinese hamsters. OGTT was performed after 12-h fasting and hamsters were given glucose orally (10 g/kg) by a gavage needle. After glucose administration, blood glucose levels **a** were measured at 0, 30, 60, and 120 min, serum insulin levels **c** were measured at 0, 15, 30, and 60 min. Area under the curve (AUC) of glucose **b** and serum insulin **d** during the OGTT was also calculated. ITT was performed by insulin intraperitoneal injection (0.75 IU/kg) after 5-h fasting. Blood glucose levels **e** were measured at 0, 30, 60, 120, and 180 min after injection. Statistical differences were analyzed by independent samples *t*-test. Data are shown as mean ± SD. Control, $n = 12$; diabetic, $n = 9$. Diabetic vs. Control: $^{*}P < 0.05$, $^{**}P < 0.01$, $^{***}P < 0.001$

of diabetic hamsters, GLUT4 mRNA and protein levels were lower than in the controls (Fig. 5c). In the liver, GLUT4 expression increased at the mRNA level, but showed a near-significant decreasing trend at the protein level in diabetic hamsters ($P = 0.053$; Fig. 5d). Immunohistochemistry of GLUT4 in liver showed similar results ($P = 0.058$; Online Resource 2a, b). Similarly, a trend for a lower level of GLUT2 was observed in the liver of diabetic hamsters (Online Resource 2c). In addition, Akt (Fig. 5e) and PPARγ (Fig. 5f) mRNA and protein level in skeletal muscle and PPARγ protein level in liver (Fig. 5g) were significantly higher in diabetic hamsters. Leptin protein expression was significantly greater in both skeletal muscle and liver of diabetic hamsters (Fig. 5h, i). These results suggested that diabetes-related genes may have contributed to the diabetic phenotypes in this animal model.

Discussion

T2DM in humans is a complex polygenic disease and is often associated with insulin resistance and defects in glucose utilization. The progression of diabetes in the strain of Chinese hamsters investigated in this study closely resembled features of human T2DM in terms of spontaneous disease development and individual metabolic profiles.

Aberrations in indicators of glucose metabolism, including FBG and PBG, were significantly higher in diabetic hamsters compared with the control group. HbA1c, a well-established clinical marker of glycemic control, increased along with FBG and PBG. In addition, OGTT indicated that the diabetic hamsters were glucose intolerant. Impaired glucose tolerance is considered to be a precursor for the development of T2DM in humans [18]. Progression from glucose intolerance to diabetes is related to inadequate insulin secretion or the degree of insulin sensitivity in response to glucose [30].

Higher fasting serum insulin level and lower insulin sensitivity were detected in the diabetic hamsters. Immunohistochemical analysis of insulin in islet cells showed that insulin granules could be clearly seen in diabetic individuals, suggesting that the islet β cells of diabetic hamsters retained the ability to synthesize and release insulin in response to glucose, whereas HOMA-IR indicated that diabetic hamsters were insulin resistant. During OGTT, the control group exhibited significantly lower serum insulin level than the diabetic hamsters at 30 min. This indicates that insulin resistance in diabetic hamsters was primarily induced by decreased insulin sensitivity, with unaddressed high blood glucose leading to continuous and burdensome stimulation of the islet β cells. The mild injury and atrophy, as well as lymphocytic

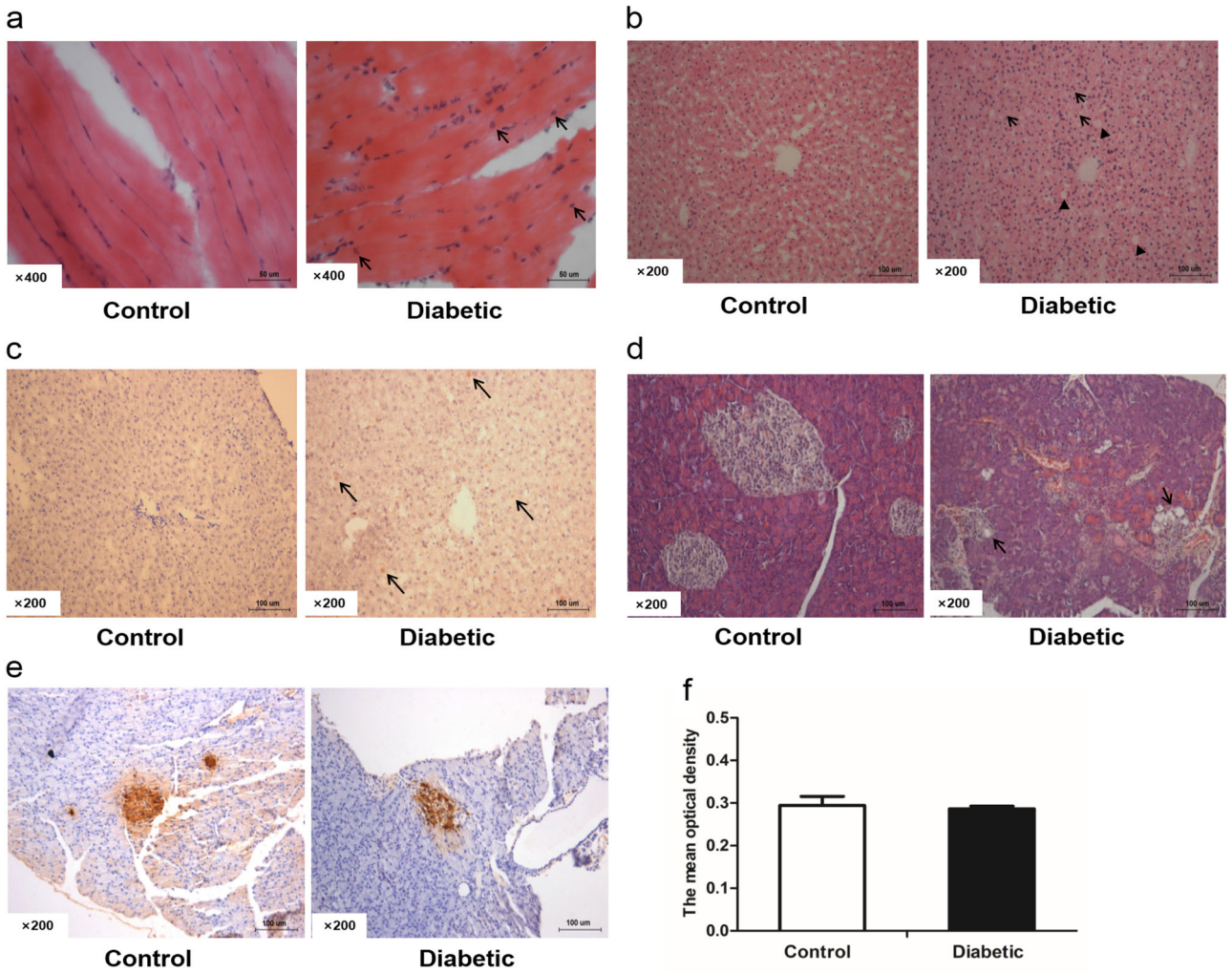

Fig. 4 Pathological analysis of target organs between control ($n = 8$) and diabetic ($n = 6$) group: skeletal muscle **a**, liver **b, c**, and pancreas **d, e, f**. **a** Hematoxylin and eosin (HE) stain of skeletal muscle (×400) showed partial cell nucleus inward migration in the diabetic hamsters (arrows). **b** HE stain of liver (×200) showed partial hepatic steatosis (arrows) and focal necrosis (arrow heads) in diabetic hamsters. **c** Sudan III stain of liver (×200) in diabetic hamsters showed a orange-red deposition (arrows) of lipids. **d** HE stain of pancreas (×200) showed mild injury of islet, maldistribution of islet cells, partial nuclear shrinkage, and occasional vacuolation (arrows) in diabetic hamsters. **e** Photomicrographs of pancreatic tissue in immunohistochemistry (200×) of insulin. The distribution of insulin in diabetic hamsters was not uniform, but the insulin granule could be clearly seen after staining. **f** The mean optical density of insulin in pancreas. Scale bar, 50 μm or 100 μm. Statistical differences were analyzed by independent samples *t*-test. Data are shown as mean ± SD. Diabetic vs. Control: $^{*}P < 0.05$, $^{**}P < 0.01$, $^{***}P < 0.001$

infiltration, seen in and around the islet cells was indicative of chronic overstimulation.

Abnormal lipid metabolism is also associated with diabetes, and fasting hypertriglyceridemia was observed in diabetic hamsters. Normal levels of TGs are associated with lower fasting glucose levels and improved insulin sensitivity [31]. Roden et al. [32] reported that intravenous administration of a TG emulsion to healthy individuals can reduce muscle glycogen synthesis and the rate of glucose uptake. It is therefore possible that the occurrence of severe hypertriglyceridemia precedes hyperglycemia and might even contribute to the development of diabetes in these hamster models, but this remains to be tested.

In general, metabolic disturbance will result in altered BMI and body composition (including BMC, BMD, fat and muscle content, among others). BMI is often used as an indicator of an individual's risk of obesity-related illnesses. In both male and female hamsters in the diabetic group, BMI decreased significantly. Body composition is a risk factor for numerous conditions such as diabetes and heart disease [33, 34]. In diabetic hamsters, the overall percentage of body fat mass and fat in tissues were markedly decreased, whereas the percentage of lean tissue significantly increased. Together, these BMI and body composition results established that these spontaneous T2DM hamsters represent a non-obese animal model. Several animal models

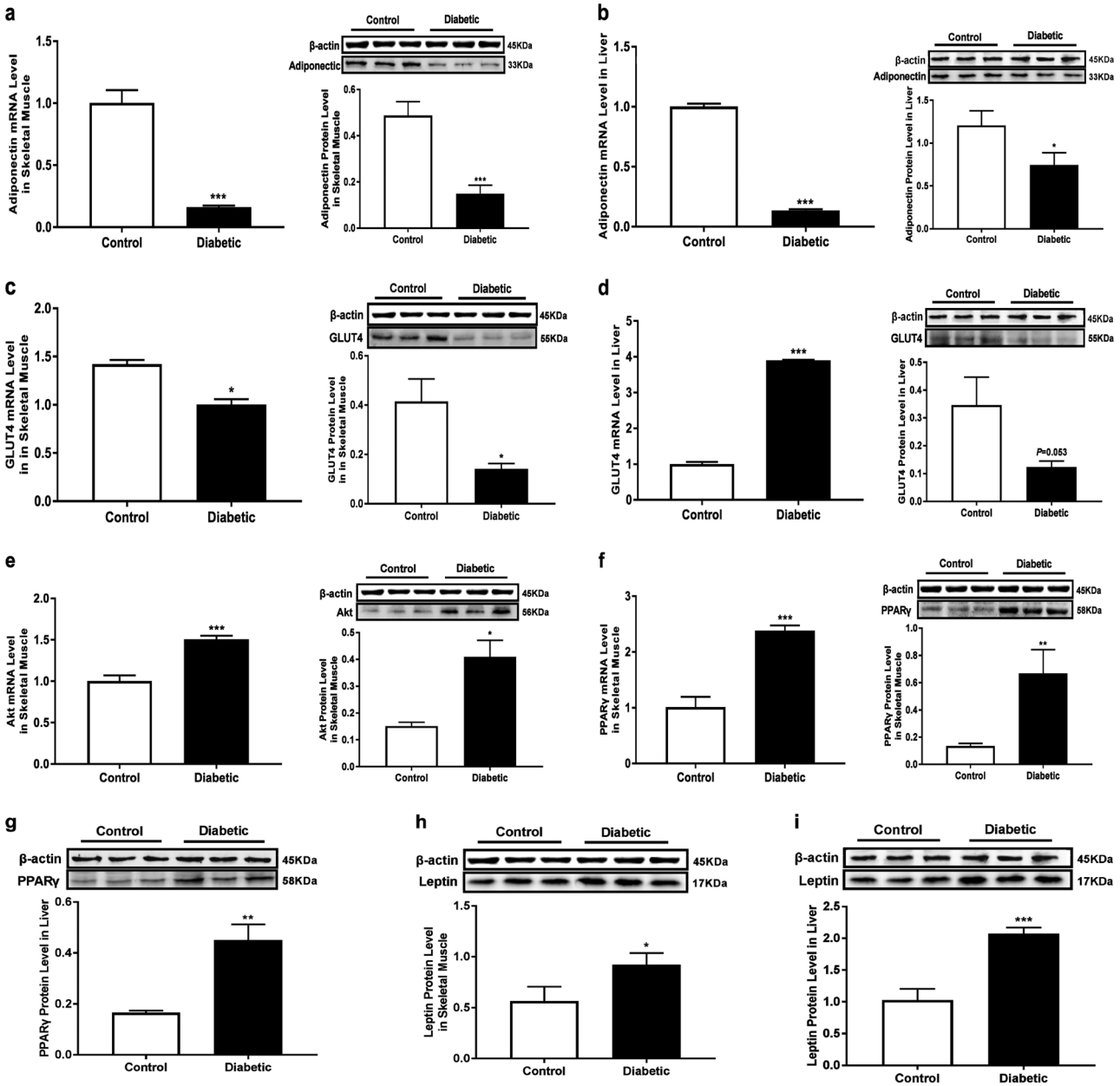

Fig. 5 Expression of candidate genes in skeletal muscle and liver of control and diabetic hamsters by RT-qPCR and western blot. **a** Adiponectin mRNA and protein expression levels in skeletal muscle. **b** Adiponectin mRNA and protein expression levels in liver. **c** GLUT4 mRNA and protein expression levels in skeletal muscle. **d** GLUT4 mRNA and protein expression levels in liver. **e** Akt mRNA and protein expression levels in skeletal muscle. **f** PPARγ mRNA and protein expression levels in skeletal muscle. **g** PPARγ protein expression level in liver. **h** Leptin protein expression level in skeletal muscle. **i** Leptin protein expression level in liver. Statistical differences were analyzed by independent samples *t*-test. Data are mean ± SD, $n = 9$ per group. Diabetic vs. Control: $^{*}P < 0.05$, $^{**}P < 0.01$, $^{***}P < 0.001$

of T2DM have been reported, including TSOD mice, which develop T2DM with severe obesity [14]; NSY mice, which develop diabetes with moderate obesity and/or severe hyperinsulinemia [13]; and TH mice and gerbils, which also show some degree of obesity when developing T2DM [15, 16]. Like GK rats, our spontaneous T2DM hamster strain represents a non-obese diabetes model [35, 36]. However, T2DM in GK rats is caused by defective insulin secretion, while Chinese hamsters in the current study exhibited insulin resistance. Therefore, this hamster model has potential scientific value for the study of non-obese T2DM caused by insulin resistance. Further studies are needed to determine the molecular mechanisms behind the decreased fat content in non-obese diabetic hamsters.

T2DM can affect physiological functions and metabolic processes in some peripheral tissues and target organs. In

the diabetic hamsters in this study, this was evident in the form of damage observed histologically in the pancreas, skeletal muscle, and liver. Mild injury and abnormal distribution of pancreatic islet cells is characteristic of diabetes [37] and were observed in the diabetic hamsters; however, insulin secretion was unimpaired, suggesting insulin resistance. Skeletal muscle, as the tissue responsible for the bulk of glucose absorption and fatty acid oxidation, plays an important role in the totality of glucose metabolism [38]. The liver also participates in glucose metabolism and has important influence on the storage, distribution, and regulation of its levels in the blood [39]. In the diabetic group, we observed inward migration of cell nuclei in skeletal muscle and deposition of lipids in the liver, which may have been associated with fasting hyperglycemia and impaired glucolipid metabolism. In addition, compared with the control group, liver glycogen was significantly increased in diabetic hamsters. This result indicated abnormal regulation of glucose in the liver, and this phenomenon may be related to insulin resistance in the liver. More research is needed to explore the molecular characteristics of the defective tissues in diabetic hamsters to further understand the causative mechanisms underlying this T2DM model.

To explore the molecular characteristics of the diabetic phenotype, we measured the expression of adiponectin, leptin, GLUT2, GLUT4, PPARγ, and Akt, which are associated with metabolic disorders. These results showed that the expression levels of both adiponectin mRNA and protein were reduced in liver and skeletal muscle, whereas leptin expression increased at the protein level. Leptin and adiponectin are important factors in the regulation of lipid metabolism and blood glucose homeostasis [40, 41]. Minokoshi et al. [42] and Yamauchi et al. [43] both reported that leptin and adiponectin regulate fatty acid oxidation by activating AMP-activated protein kinase in skeletal muscle. Adiponectin is an insulin-sensitizing hormone, and severely low levels can cause lipid accumulation in non-adipose tissues such as the liver. This can cause functional impairments known as lipotoxicity [18]. In addition, PPARγ serves as a key regulator of adipocyte differentiation and lipid and carbohydrate metabolism [19]. In diabetic hamsters, PPARγ was increasingly expressed in both liver and skeletal muscle. Yu et al. [44] reported that a high level of PPARγ is needed to induce lipogenesis and lipid accumulation in mouse liver. Our results indicate that liver steatosis may be related to the increased expression of PPARγ in liver of diabetic hamsters. Although further studies are needed, we speculate that spontaneous diabetes in hamsters may be associated with altered expression of leptin, adiponectin, and PPARγ.

Impaired glucose uptake in skeletal muscle may be explained by the reduced GLUT4 level and/or changes in its translocation to the plasma membrane [30]. In the basal condition, GLUT4 protein remains in specialized vesicles within the cell [23]. When post-prandial glucose levels rise, insulin receptor signal transduction is activated and GLUT4 protein is translocated to the plasma membrane, thus completing the transport of glucose and reducing blood glucose concentration [23, 30]. Miura et al. [45] have reported that impaired GLUT4 translocation in skeletal muscle is partly responsible for insulin resistance. Meanwhile, PI3K/Akt is an important signaling pathway for GLUT4 translocation by regulating insulin stimulation [24]. In diabetic hamsters, Akt mRNA and protein expression increased, whereas the levels of GLUT4 decreased in the skeletal muscle. However, there were no significant changes in protein expression of GLUT4, or Akt in the liver. Hence, it is possible that the translocation of GLUT4 is defective in diabetic hamsters, which may be correlated with the expression of Akt in skeletal muscle. The specific relationship between the PI3K/Akt signaling pathway remains to be investigated.

In summary, we have established a spontaneous diabetic hamster model for non-obese T2DM. Metabolic abnormalities in Chinese hamster diabetic models are similar to those observed in human T2DM, which makes this model a valuable resource for studying the molecular mechanisms underlying this condition.

Funding This study was funded by the Shanxi Province Experimental Animal Resources Service Platform of China (no. 201605D121019), the Shanxi Scholarship Council of China (no. 2015-054), and the Shanxi Medical University Youth Fund Project of China (no. 02201317).

Compliance with ethical standards

Conflict of interest The authors declare that they have no conflict of interest.

Ethical approval All applicable institutional guidelines for the care and use of animals were followed.

References

1. S.Y. Lu, S.D. Qi, Y. Zhao, Y.Y. Li, F.M. Yang, W.H. Yu, M. Jin, L.X. Chen, J.B. Wang, Z.L. He, H.J. Li, Type 2 diabetes mellitus non-genetic Rhesus monkey model induced by high fat and high sucrose diet. Exp. Clin. Endocrinol. Diabetes. **123**(1), 19–26 (2015). https://doi.org/10.1055/s-0034-1385923
2. B.K. Podell, D.F. Ackart, M.A. Richardson, J.E. DiLisio, B. Pulford, R.J. Basaraba, A model of type 2 diabetes in the guinea pig using sequential diet-induced glucose intolerance and streptozotocin treatment. Dis. Models Mech. **10**(2), 151–162 (2017). https://doi.org/10.1242/dmm.025593
3. N.H. Cho, J.E. Shaw, S. Karuranga, Y. Huang, J.D. da Rocha Fernandes, A.W. Ohlrogge, B. Malanda, IDF Diabetes Atlas:

global estimates of diabetes prevalence for 2017 and projections for 2045. Diabetes Res. Clin. Pract. **138**, 271–281 (2018). https://doi.org/10.1016/j.diabres.2018.02.023
4. X. Li, J. Lu, Y. Wang, X. Huo, Z. Li, S. Zhang, C. Li, M. Guo, X. Du, Z. Chen, Establishment and characterization of a newly established diabetic gerbil line. PLoS ONE **11**(7), e0159420 (2016). https://doi.org/10.1371/journal.pone.0159420
5. N. Lawlor, J. George, M. Bolisetty, R. Kursawe, L. Sun, Single cell transcriptomes identify human islet cell signatures and reveal cell-type-specific expression changes in type 2 diabetes. Genome Res. **27**(2), 208 (2017)
6. C. Sandor, N.L. Beer, C. Webber, Diverse type 2 diabetes genetic risk factors functionally converge in a phenotype-focused gene network. PLoS Comput. Biol. **13**(10), e1005816 (2017). https://doi.org/10.1371/journal.pcbi.1005816
7. S. De Rosa, B. Arcidiacono, E. Chiefari, A. Brunetti, C. Indolfi, D.P. Foti, Type 2 diabetes mellitus and cardiovascular disease: genetic and epigenetic links. Front. Endocrinol. **9**, 2 (2018). https://doi.org/10.3389/fendo.2018.00002
8. S. O'Rahilly, I. Barroso, N.J. Wareham, Genetic factors in type 2 diabetes: the end of the beginning? Science **307**(5708), 370–373 (2005)
9. W.T. Cefalu, Animal models of type 2 diabetes: clinical presentation and pathophysiological relevance to the human condition. Ilar J. **47**(3), 186–198 (2006)
10. M.S. Islam, R.D. Wilson, Experimentally induced rodent models of type 2 diabetes. Methods Mol. Biol. **933**, 161 (2012)
11. A. Nishigaki, H. Noma, T. Kakizawa, The relations between doses of streptozotocin and pathosis in induced diabetes mellitus. Shikwa Gakuho **89**(3), 639–662 (1989)
12. D.A. Rees, J.C. Alcolado, Animal models of diabetes mellitus. Diabet. Med. **22**(4), 359–370 (2010)
13. H. Ueda, H. Ikegami, E. Yamato, J. Fu, M. Fukuda, G. Shen, The NSY mouse: a new animal model of spontaneous NIDDM with moderate obesity. Diabetologia **38**(5), 503–508 (1995)
14. W. Suzuki, S. Iizuka, M. Tabuchi, S. Funo, T. Yanagisawa, M. Kimura, A new mouse model of spontaneous diabetes derived from ddY strain. Exp. Anim. **48**(3), 181–189 (1999)
15. J.H. Kim, A.M. Saxton, The TALLYHO mouse as a model of human type 2 diabetes. Methods Mol. Biol. (Clifton, N. J.) **933**, 75–87 (2012). https://doi.org/10.1007/978-1-62703-068-7_6
16. L. Boquist, Obesity and pancreatic islet hyperplasia in the Mongolian gerbil. Diabetologia **8**(4), 274–282 (1972)
17. K. Kimura, T. Toyota, M. Kakizaki, M. Kudo, K. Takebe, Y. Goto, Impaired insulin secretion in the spontaneous diabetes rats. Tohoku J. Exp. Med. **137**(4), 453–459 (1982)
18. S.E. Kahn, R.L. Hull, K.M. Utzschneider, Mechanisms linking obesity to insulin resistance and type 2 diabetes. Nature **444** (7121), 840–846 (2006). https://doi.org/10.1038/nature05482
19. R. Raj, J.S. Bhatti, S.K. Bhadada, P.W. Ramteke, Association of polymorphisms of peroxisome proliferator activated receptors in early and late onset of type 2 diabetes mellitus. Diabetes Metab. Syndr. **11**(Suppl 1), S287–s293 (2017). https://doi.org/10.1016/j.dsx.2017.03.004
20. T.J. Hsiao, E. Lin, The Pro12Ala polymorphism in the peroxisome proliferator-activated receptor gamma (PPARG) gene in relation to obesity and metabolic phenotypes in a Taiwanese population. Endocrine **48**(3), 786–793 (2015). https://doi.org/10.1007/s12020-014-0407-7
21. X. Lv, L. Zhang, J. Sun, Z. Cai, Q. Gu, R. Zhang, A. Shan, Interaction between peroxisome proliferator-activated receptor gamma polymorphism and obesity on type 2 diabetes in a Chinese Han population. Diabetol. Metab. Syndr. **9**, 7 (2017). https://doi.org/10.1186/s13098-017-0205-5
22. M. Mueckler, Family of glucose-transporter genes. Implications for glucose homeostasis and diabetes. Diabetes **39**(1), 6–11 (1990)
23. X. Zhou, P. Shentu, Y. Xu, Spatiotemporal regulators for insulin-stimulated GLUT4 vesicle exocytosis. J. Diabetes Res. **2017**, 1683678 (2017). https://doi.org/10.1155/2017/1683678
24. M. Beg, N. Abdullah, F.S. Thowfeik, N.K. Altorki, T.E. Mcgraw, Distinct Akt phosphorylation states are required for insulin regulated Glut4 and Glut1-mediated glucose uptake. eLife **6**(2017-05-22), (2017)
25. W. Andreas, C.B. Wollheim, Minireview: implication of mitochondria in insulin secretion and action. Endocrinology **147**(6), 2643–2649 (2006)
26. H. Meier, G.A. Yerganian, Spontaneous hereditary diabetes mellitus in Chinese hamster (*Cricetulus griseus*). 1. Pathological findings. Proc. Soc. Exp. Biol. Med **100**(4), 810–815 (1959)
27. H. Meier, G. Yerganian, Spontaneous diabetes mellitus in the Chinese hamster (*Cricetulus griseus*). II. Findings in the offspring of diabetic parents. Diabetes **10**(1), 12 (1961)
28. H. Meier, G. Yerganian, Spontaneous hereditary diabetes mellitus in the Chinese hamster (*Cricetulus griseus*). III. Maintenance of a diabetic hamster colony with the aid of hypoglycemic therapy. Diabetes **10**, 19–21 (1961)
29. S. Andrikopoulos, A.R. Blair, N. Deluca, B.C. Fam, J. Proietto, Evaluating the glucose tolerance test in mice. Am. J. Physiol. Endocrinol. Metab. **295**(6), E1323 (2008). https://doi.org/10.1152/ajpendo.90617.2008
30. J.H. Kim, T.P. Stewart, M. Soltani-Bejnood, L. Wang, J.M. Fortuna, O.A. Mostafa, N. Moustaid-Moussa, A.M. Shoieb, M.F. McEntee, Y. Wang, L. Bechtel, J.K. Naggert, Phenotypic characterization of polygenic type 2 diabetes in TALLYHO/JngJ mice. J. Endocrinol. **191**(2), 437–446 (2006). https://doi.org/10.1677/joe.1.06647
31. G. Mingrone, F.L. Henriksen, A.V. Greco, L.N. Krogh, E. Capristo, A. Gastaldelli, M. Castagneto, E. Ferrannini, G. Gasbarrini, H. Beck-Nielsen, Triglyceride-induced diabetes associated with familial lipoprotein lipase deficiency. Diabetes **48**(6), 1258–1263 (1999). https://doi.org/10.2337/diabetes.48.6.1258
32. M. Roden, T.B. Price, G. Perseghin, K.F. Petersen, D.L. Rothman, G.W. Cline, G.I. Shulman, Mechanism of free fatty acid-induced insulin resistance in humans. J. Clin. Investig. **97**(12), 2859–2865 (1996). https://doi.org/10.1172/jci118742
33. Z. Abdeen, C. Jildeh, S. Dkeideek, R. Qasrawi, I. Ghannam, H. Al Sabbah, Overweight and obesity among Palestinian adults: analyses of the anthropometric data from the First National Health and Nutrition Survey (1999-2000). J. Obes. **2012**, 213547 (2012). https://doi.org/10.1155/2012/213547
34. M.M. Lima-Martinez, M. Paoli, M. Rodney, N. Balladares, M. Contreras, L. D'Marco, G. Iacobellis, Effect of sitagliptin on epicardial fat thickness in subjects with type 2 diabetes and obesity: a pilot study. Endocrine **51**(3), 448–455 (2016). https://doi.org/10.1007/s12020-015-0710-y
35. Y. Goto, M. Kakizaki, N. Masaki, Production of spontaneous diabetic rats by repetition of selective breeding. Tohoku J. Exp. Med. **119**(1), 85–90 (1976)
36. G. Miao, T. Ito, F. Uchikoshi, M. Tanemura, K. Kawamoto, K. Shimada, M. Nozawa, H. Matsuda, Development of islet-like cell clusters after pancreas transplantation in the spontaneously diabetic Torri rat. Am. J. Transplant. **5**(10), 2360–2367 (2005). https://doi.org/10.1111/j.1600-6143.2005.01023.x
37. A. Charollais, A. Gjinovci, J. Huarte, J. Bauquis, A. Nadal, F. MartãN, Junctional communication of pancreatic beta cells contributes to the control of insulin secretion and glucose tolerance. J. Clin. Investig. **106**(2), 235–243 (2000)
38. A.K. Turpeinen, T.O. Takala, P. Nuutila, T. Axelin, M. Luotolahti, M. Haaparanta, J. Bergman, H. Hamalainen, H. Iida, M. Maki, M.I. Uusitupa, J. Knuuti, Impaired free fatty acid uptake in skeletal muscle but not in myocardium in patients with impaired glucose tolerance: studies with PET and 14(R,S)-[18F]fluoro-6-

thia-heptadecanoic acid. Diabetes **48**(6), 1245–1250 (1999). https://doi.org/10.2337/diabetes.48.6.1245
39. E.S. Jin, M. Szuszkiewicz-Garcia, J.D. Browning, J.D. Baxter, N. Abate, C.R. Malloy, Influence of liver triglycerides on suppression of glucose production by insulin in men. J. Clin. Endocrinol. Metab. **100**(1), 235–243 (2015). https://doi.org/10.1210/jc.2014-2404
40. A.H. Bakker, J. Nijhuis, W.A. Buurman, F.M. van Dielen, J.W. Greve, Low number of omental preadipocytes with high leptin and low adiponectin secretion is associated with high fasting plasma glucose levels in obese subjects. Diabetes Obes. Metab. **8**(5), 585–588 (2006). https://doi.org/10.1111/j.1463-1326.2006.00558.x
41. G. Paltoglou, M. Schoina, G. Valsamakis, N. Salakos, A. Avloniti, A. Chatzinikolaou, A. Margeli, C. Skevaki, M. Papagianni, C. Kanaka-Gantenbein, I. Papassotiriou, G.P. Chrousos, I.G. Fatouros, G. Mastorakos, Interrelations among the adipocytokines leptin and adiponectin, oxidative stress and aseptic inflammation markers in pre- and early-pubertal normal-weight and obese boys. Endocrine **55**(3), 925–933 (2017). https://doi.org/10.1007/s12020-017-1227-3
42. Y. Minokoshi, Y.B. Kim, O.D. Peroni, L.G. Fryer, C. Mã¼Ller, D. Carling, Leptin stimulates fatty-acid oxidation by activating AMP-activated protein kinase. Nature **415**(6869), 339–343 (2002)
43. T. Yamauchi, J. Kamon, Y. Minokoshi, Y. Ito, H. Waki, S. Uchida, S. Yamashita, M. Noda, S. Kita, K. Ueki, K. Eto, Y. Akanuma, P. Froguel, F. Foufelle, P. Ferre, D. Carling, S. Kimura, R. Nagai, B.B. Kahn, T. Kadowaki, Adiponectin stimulates glucose utilization and fatty-acid oxidation by activating AMP-activated protein kinase. Nat. Med. **8**(11), 1288–1295 (2002). https://doi.org/10.1038/nm788
44. S. Yu, K. Matsusue, P. Kashireddy, W.Q. Cao, V. Yeldandi, A.V. Yeldandi, Adipocyte-specific gene expression and adipogenic steatosis in the mouse liver due to peroxisome proliferator-activated receptorgamma1 (PPARgamma1) overexpression. J. Biol. Chem. **278**(1), 498–505 (2003)
45. T. Miura, W. Suzuki, E. Ishihara, I. Arai, H. Ishida, Y. Seino, Impairment of insulin-stimulated GLUT4 translocation in skeletal muscle and adipose tissue in the Tsumura Suzuki obese diabetic mouse: a new genetic animal model of type 2 diabetes. Eur. J. Endocrinol. **145**(6), 785 (2001)